Compact Antenna Spacing in mmWave MIMO Systems Using Random Phase Precoding

G. D. Surabhi and A. Chockalingam
Department of ECE, Indian Institute of Science, Bangalore 560012

***Abstract*—Presence of strong line of sight (LOS) components in multiple-input multiple-output (MIMO) systems operating at mmWave frequencies result in ill-conditioned channel matrices. However, optimum inter-antenna spacing can result in orthogonal channel matrices under LOS conditions. This optimal spacing is typically large (of the order of tens of wavelengths). Antennas separated by less than optimal spacing result in degraded performance due to high spatial correlation. This motivates the need to investigate techniques that can reduce the spacing without compromising much in performance. In this work, we propose *random phase precoding (RPP)* as an attractive method to achieve this objective. Our contributions in this paper are two-fold. First, RPP for reducing inter-antenna spacing in mmWave communications is novel and has not been reported before. Our results show that, using RPP, the inter-antenna spacing can be reduced to the order of wavelength (5mm at 60 GHz frequency) compared to optimal spacing which is of the order of tens of wavelengths. This is achieved without the need for channel state information at the transmitter. We also present an analysis that shows that RPP reduces the effective correlation which, in turn, aids compact spacing. Second, we study an index modulation scheme where the random phase precoder matrices are indexed to convey additional information bits. The indexed RPP scheme is found to perform better than the non-indexed RPP scheme.**

Keywords *– mmWave MIMO communication, inter-antenna spacing, spatial correlation, random phase precoding.*

I. Introduction

The design of wireless links that operate in mmWave frequencies has gained significant interest due to the demand for high data rates and the availability of 7 GHz of unlicensed spectrum around 60 GHz [1], [2]. The small wavelengths associated with mmWaves (e.g., 5mm at 60 GHz carrier frequency) allow the use of a large number of antenna elements packed in small form factors [3]. The propagation at mmWave frequencies is dominated by strong line-of-sight (LOS) component. A consequence of this is that mmWave MIMO channels are characterized by high spatial correlation. This can result in badly conditioned channel matrices. Proper placement of antenna elements can alleviate this problem. For example, it is possible to make the mmWave LOS MIMO channel matrix to be orthogonal in uniform linear arrays (ULA) through optimum inter-antenna spacing [4], [5]. Several papers that study the performance of mmWave MIMO systems assume this optimum spacing [6]- [9]. However, the optimum spacing is typically large (of the order of several wavelengths). When the spacing used is less than the optimum spacing, the channel becomes increasingly spatially correlated, which, in turn, degrades performance [10]. This motivates the need to investigate techniques that can reduce the spacing without compromising much in performance. This forms the main focus of this paper. The approach we propose in this paper to achieve this objective is *random phase precoding*.

In random phase precoding (RPP), the transmit signal vector is pre-multiplied with a precoder matrix whose entries are random phases which are known to the receiver for decoding purposes [11]. The pre-multiplication essentially creates diversity opportunity by allowing a data symbol to be present in multiple channel uses, and joint detection over these channel uses results in improved performance.

Our first contribution in this paper is that we propose RPP as an attractive method to achieve compact antenna spacing in mmWave MIMO communications. To our knowledge, this novel idea has not been reported before. Our simulation results show that with RPP, the inter-antenna spacing can be reduced to the order of wavelength from the optimal spacing which is of the order of tens of wavelengths. For example, a $\lambda/2$-spaced array (i.e., 2.5 mm spacing at 60 GHz carrier frequency) employing RPP achieves a performance within 2.3 dB of the optimally spaced array performance (where the optimal spacing is 86.6 mm) in LOS channels at 10^{-5} BER, and within 0.5 dB in Rician channels with 10 dB Rician factor. It is interesting to note that this performance is achieved without the need for channel state information at the transmitter. We also present an analysis which explains why RPP achieves this good performance with reduced spacing. The second contribution is that we study an *indexed RPP* scheme where a set of predefined RPP matrices are indexed to convey additional information bits [12]. Simulation results show that, compared to the non-indexed RPP scheme, the indexed RPP scheme performs better by about 9 dB in LOS channels and about 3 dB in Rician channels with 10 dB Rician factor at 10^{-5} BER.

The rest of this paper is organized as follows. The mmWave system and channel models are presented in Sec. II. The RPP scheme and its performance in mmWave MIMO systems with compact antenna spacing are presented in Sec. III. Indexed RPP scheme and its performance are presented in Sec. IV. Conclusions are presented in Sec. V.

II. System model

Consider an mmWave MIMO system with N_t transmit and N_r receive antennas in uniform linear array (ULA) configuration as shown in Fig. 1. Let $\mathbf{H}$ denote the $N_r \times N_t$ MIMO channel matrix. Assuming perfect synchronization, the $N_r \times 1$ received signal vector at the receiver is given by

$$\mathbf{y} = \mathbf{H}\mathbf{x} + \mathbf{n}, \tag{1}$$

where $\mathbf{y} \in \mathbb{C}^{N_r}$ is the received signal vector, $\mathbf{H} \in \mathbb{C}^{N_r \times N_t}$ is the channel matrix, $\mathbf{x} \in \mathbb{C}^{N_t}$ is the transmitted signal vector,

This work was supported in part by the J. C. Bose National Fellowship, Department of Science and Technology, Government of India.

978-1-5090-5935-5/17/$31.00 ©2017 IEEE

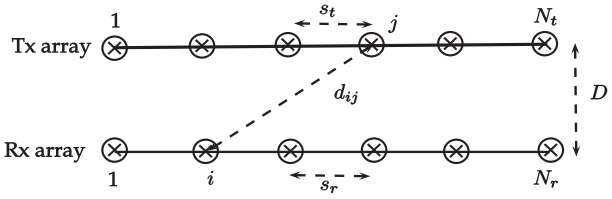

Fig. 1. mmWave MIMO system.

and $\mathbf{n} \sim \mathcal{CN}(\mathbf{0}, \sigma^2\mathbf{I})$. A frequency-flat Rician channel model is assumed, where the $\mathbf{H}$ matrix can be written in the form

$$\mathbf{H} = \sqrt{\frac{K}{K+1}}\mathbf{H}_{\text{LOS}} + \sqrt{\frac{1}{K+1}}\mathbf{H}_{\text{NLOS}}, \tag{2}$$

where $\mathbf{H}_{\text{LOS}}$ and $\mathbf{H}_{\text{NLOS}}$ denote the LOS and non-LOS component matrices, respectively, and K is the Rician factor, defined as the ratio of the powers in the LOS and non-LOS components. Note that $K = \infty$ corresponds to the case of pure LOS channel and $K = 0$ corresponds to the case of Rayleigh fading channel. The entry in the ith row and jth column of $\mathbf{H}_{\text{LOS}}$ is given by $e^{-j\frac{2\pi}{\lambda}d_{ij}}$, where d_{ij} denotes the LOS path length between the jth transmit antenna and the ith receive antenna, and λ is the wavelength. The entries of the $\mathbf{H}_{\text{NLOS}}$ are assumed to be i.i.d and distributed as $\mathcal{CN}(0, 1)$.

A. Optimal inter-antenna spacing

Let s_t denote the inter-antenna spacing in the ULA at the transmitter (see Fig. 1). Likewise, let s_r denote the inter-antenna spacing in the ULA at the receiver. Let D denote the distance between the transmitter and the receiver. In the pure LOS channel (i.e., $K = \infty$), the channel matrix $\mathbf{H}$ $(= \mathbf{H}_{\text{LOS}})$ becomes orthogonal if the condition

$$\langle \mathbf{h}_i, \mathbf{h}_j \rangle = 0, \ \forall i \neq j \tag{3}$$

is satisfied, where $\mathbf{h}_i$ denotes the ith column of $\mathbf{H}$. It has been shown that the optimum s_t and s_r that satisfy the above condition for a ULA is given by [4], [5]

$$s_t s_r \approx \frac{(2n+1)D\lambda}{M}, \quad n \in \mathbb{Z}^+, \tag{4}$$

where $M = \max(N_t, N_r)$. When s_t and s_r are equal, then $s_t = s_r = s$ becomes

$$s \approx \sqrt{\frac{(2n+1)D\lambda}{M}}, \quad n \in \mathbb{Z}^+. \tag{5}$$

Note that the condition in (3) is satisfied for $n = 0, 1, 2, \cdots$, and the minimum optimum spacing corresponds to $n = 0$ in (4), (5). Also, note that the optimum array length at the transmitter is given by $(N_t - 1)s$, which increases with increased N_t. Likewise, $(N_r - 1)s$ is the optimum array length at the receiver.

1) An example scenario: Consider a 2×2 MIMO system operating at 60 GHz ($\lambda = 5$ mm), where the transmit and receive arrays are separated by a distance $D = 3$ m. Assume that the inter-antenna separation at the transmitter and receiver arrays are equal (i.e., $s_t = s_r = s$). Then, from (5) with $n = 0$, an optimum inter-antenna spacing of 86.6 mm is required for $\mathbf{H}$ to be orthogonal. Note that this optimum spacing is about 17λ. Contrast this with the operation in 2.4 GHz or 5 GHz bands under rich scattering, where $\lambda/2$ separation is adequate to achieve independence among the entries in the channel matrix.

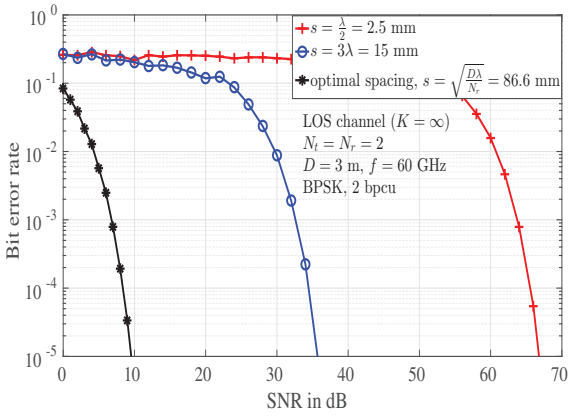

Fig. 2. Comparison of the BER performance of 2×2 mmWave MIMO system at 60 GHz with $D = 3$ m under i) optimal spacing, ii) 3λ spacing, and iii) $\lambda/2$ spacing in LOS channel.

B. Effect of suboptimum spacing on performance

In this subsection, we present an illustration of the degrading effect of suboptimum spacing on the BER performance. Figure 2 shows the BER performance of a 2×2 MIMO system operating at 60 GHz with $D = 3$ m and BPSK modulation. The optimum spacing in this case is $s = 17.32\lambda = 86.6$ mm. LOS channel ($K = \infty$) is considered. The BER performance with optimum spacing ($17.32\lambda = 86.6$ mm), 3λ spacing (15 mm), and $\lambda/2$ spacing (2.5 mm) are plotted. As expected, it can be seen that the best BER performance is achieved with optimum spacing. As the spacing is reduced, the BER performance significantly degrades. For example, at a BER of 10^{-5}, the performance of 3λ spacing is worse by about 26 dB compared to that of the optimal spacing. This degradation increases further to about 58 dB if $\lambda/2$ spacing is used. This points to the potential to bridge the large performance gap between optimal spacing and $\lambda/2$ spacing. Accordingly, in the next section, we propose RPP to improve the performance of $\lambda/2$ spacing in mmWave MIMO systems.

III. Random Phase Precoding Scheme

Figure 3 shows the mmWave MIMO transmitter that employs RPP. In this RPP system, transmission is carried out using N_t antennas in p channel uses. Let $\mathbb{A}$ denote the modulation alphabet used. $N_t p$ modulated symbols from $\mathbb{A}$ form a vector $\mathbf{x}$ of length $N_t p \times 1$. This vector is precoded by an RPP matrix $\mathbf{P}$ of size $N_t p \times N_t p$. The (i, j)th entry of $\mathbf{P}$ is $\frac{1}{\sqrt{N_t p}} e^{j\theta_{ij}}$, where the θ_{ij}s are chosen from uniform distribution in the range $[-\pi, \pi)$. The θ_{ij}s are generated using a pseudo-random sequence generator, whose seed is pre-shared among the transmitter and the receiver. The precoded output vector $\mathbf{Px}$ of size $N_t p \times 1$ is transmitted in p channel uses, where in each channel use an $N_t \times 1$ subvector of $\mathbf{Px}$ is transmitted using N_t antennas. The received signal vector $\mathbf{y}$ of length $N_r p \times 1$ at the receiver can be written in the form

$$\mathbf{y} = \tilde{\mathbf{H}}\mathbf{P}\mathbf{x} + \mathbf{n}, \tag{6}$$

where $\tilde{\mathbf{H}}$ is the matrix of size $N_r p \times N_t p$, defined as $\tilde{\mathbf{H}} = \text{diag}\{\mathbf{H}_{(1)}\mathbf{H}_{(2)} \cdots \mathbf{H}_{(p)}\}$, where $\mathbf{H}_{(i)}$ is the $N_r \times N_t$ channel matrix corresponding to ith channel use, which is of the form in (2). The noise vector $\mathbf{n}$ is defined as

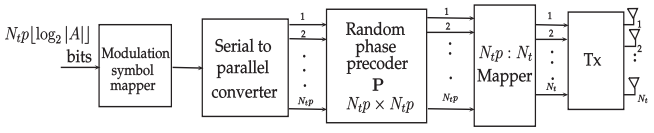

Fig. 3. mmWave MIMO transmitter with random phase precoding.

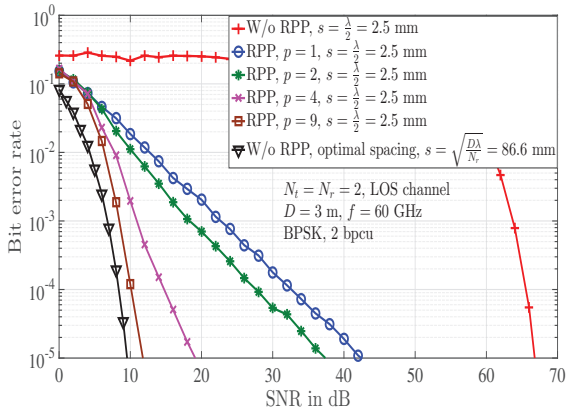

Fig. 4. BER performance of 2×2 system with RPP in LOS channel at 60 GHz with $D = 3$ m, BPSK, and ML detection.

$\mathbf{n} = [\mathbf{n}_{(1)}^T \mathbf{n}_{(2)}^T \cdots \mathbf{n}_{(p)}^T]^T$, where $\mathbf{n}_{(i)}$ is the $N_r \times 1$ noise vector corresponding to the ith channel use, whose entries are distributed as $\mathcal{CN}(0, \sigma^2)$. At the receiver, detection is carried out jointly over p channel uses. The ML detection rule is given by

$$\hat{\mathbf{x}} = \underset{\mathbf{x} \in \mathbb{A}^{N_t p}}{\operatorname{argmin}} \|\mathbf{y} - \tilde{\mathbf{H}}\mathbf{P}\mathbf{x}\|^2. \tag{7}$$

A. Performance results and discussions

In this subsection, we present the BER performance of a 2×2 MIMO system operating at 60 GHz with $D = 3$ m, BPSK modulation, and RPP under ML detection. The optimal inter-antenna spacing for this setting is $s = 86.6$ mm. We compare the BER performance of the following three settings: i) system without RPP, optimal spacing (86.6 mm), ii) system without RPP, $\lambda/2$ spacing (2.5 mm), and iii) system with RPP, $\lambda/2$ spacing (2.5 mm). Figure 4 shows this comparison for LOS channel ($K = \infty$). The performance of the system with RPP is shown for different values of p. As we saw earlier in Fig. 2, without RPP, the performance of $\lambda/2$ spacing is worse by about 58 dB at 10^{-5} BER compared to that of optimum spacing. It is interesting to see that RPP significantly improves the performance of $\lambda/2$ spacing. This improvement is increased for increased values of p. For example, RPP with $p = 9$ under $\lambda/2$ spacing performs close to optimum spacing performance by just about 2.3 dB at 10^{-5} BER. This is a drastic improvement (about 55.5 dB improvement) made possible by multiple occurrences of a symbol induced by RPP and joint detection over p channel uses. Also, the analysis in Sec. III-B shows that RPP essentially reduces the correlation in the effective channel matrix $\tilde{\mathbf{H}}\mathbf{P}$ which results in good performance even with reduced inter-antenna spacing. Note that RPP achieves this improvement without any channel state information at the transmitter.

Figure 5 shows the SNR required to achieve a BER of 10^{-3} as a function of inter-antenna spacing without and with

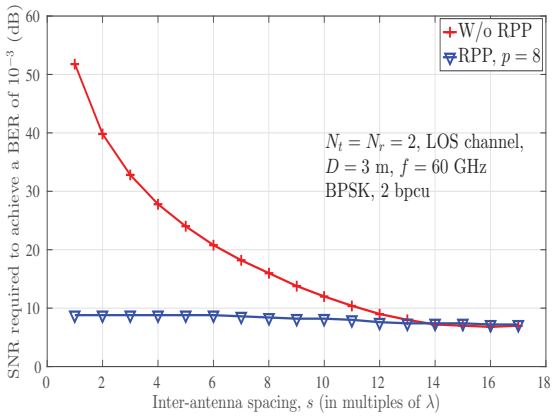

Fig. 5. Variation of SNR required to achieve a BER of 10^{-3} as a function of inter-antenna spacing s (in multiples of λ) without and with RPP in 2×2 MIMO LOS channel.

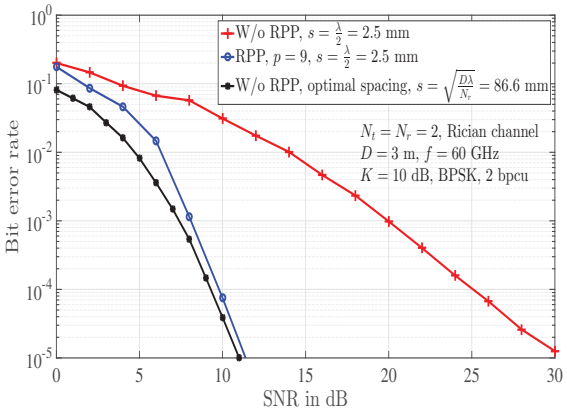

Fig. 6. BER performance of 2×2 system with RPP in Rician channel at 60 GHz with $D = 3$m, Rician factor=10 dB, $p = 9$, BPSK, and ML detection.

RPP in a 2×2 MIMO LOS channel. It is seen that the required SNR with RPP ($p = 8$) is significantly less compared to that without RPP at small inter-antenna spacings. Figure 6 shows that in a Rician channel with a Rician factor of $K = 10$ dB [13], RPP with $p = 9$ at $\lambda/2$ spacing achieves a performance close to within just 0.5 dB of the optimum spacing performance at 10^{-5} BER.

Note that within the optimum spacing of 17λ, 34 antennas spaced $\lambda/2$ apart can be placed. Using more receive antennas with $\lambda/2$ spacing along with RPP can offer additional receive dimensions and hence further performance improvement. Figure 7 illustrates this point where we have plotted the performance of RPP with $N_r = 2, 4, 8$. Denoting the lengths of the transmit and receive arrays with $\lambda/2$ spacing as l_t and l_r, respectively, the receive array lengths l_r for $N_r = 2, 4, 8$ are 2.5 mm, 7.5 mm, 17.5 mm, respectively. Note that the length of the Rx array with $N_r = 2$ and optimum inter-antenna spacing is 86.6 mm. From Fig. 7, we see that 2×4 system with $\lambda/2$ spaced array achieves a performance gain of 0.4 dB compared to 2×2 system with optimally spaced array. Note that the achieved reduction in the Tx and Rx array lengths in this case is 97.11% and 91.4%, respectively. Also, we see that 2×8 system with $\lambda/2$ spaced array and RPP outperforms optimally spaced 2×2 system by about 3 dB. This gain in performance is achieved along with 97.11% and

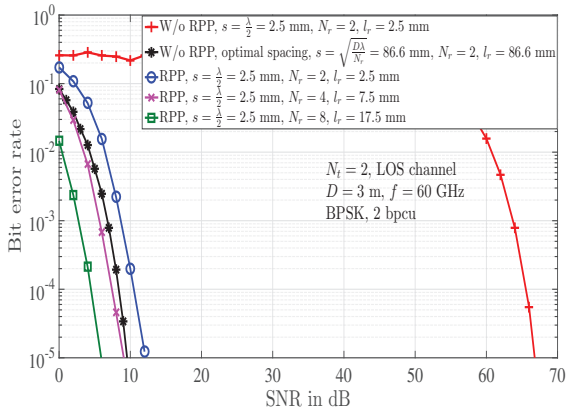

Fig. 7. BER performance comparison of $\lambda/2$ spaced MIMO systems employing RPP with $p=8$, $N_t=2$, and $N_r=2,4,8$ in LOS channel.

79.79% reduction in Tx and Rx array lengths, respectively. Hence, for a given array length, employing more receive antennas with compact spacing along with RPP can achieve improved performance.

B. Correlation analysis in RPP

In this subsection, we analyze the correlation characteristics of the effective matrix $\mathbf{G}$, defined as $\mathbf{G} \triangleq \tilde{\mathbf{H}}\mathbf{P}$, in LOS channel. With this definition, (6) can be written as

$$\mathbf{y} = \underbrace{\tilde{\mathbf{H}}\mathbf{P}}_{\triangleq\, \mathbf{G}}\mathbf{x} + \mathbf{n}. \tag{8}$$

The above system can be viewed as an $N_r p \times N_t p$ MIMO system with $\mathbf{G}$ as the effective channel matrix. The (i,j)th element of $\mathbf{G}$, denoted by g_{ij}, is given by

$$g_{ij} = \mathbf{h}_i^\dagger \mathbf{p}_j, \tag{9}$$

where $\mathbf{h}_i^\dagger$ denotes the ith row of $\tilde{\mathbf{H}}$ and $\mathbf{p}_j$ denotes the jth column of $\mathbf{P}$. Since θ_{ij}s are uniformly distributed in $[-\pi,\pi)$, $E[g_{ij}]=0$. The correlation between g_{ij} and g_{kl} is given by the correlation coefficient $\rho_{ij,kl}$, defined as

$$\rho_{ij,kl} = \frac{E[g_{ij}g_{kl}^*]}{\sqrt{E[g_{ij}g_{ij}^*]E[g_{kl}g_{kl}^*]}}, \tag{10}$$

where

$$\begin{aligned} E[g_{ij}g_{kl}^*] &= E[\mathbf{h}_i^\dagger \mathbf{p}_j \mathbf{p}_l^\dagger \mathbf{h}_k] \\ &= \mathbf{h}_i^\dagger E[\mathbf{p}_j \mathbf{p}_l^\dagger]\mathbf{h}_k. \end{aligned} \tag{11}$$

Defining $N \triangleq N_t p$, $E[\mathbf{p}_j\mathbf{p}_l^\dagger]$ can be written as

$$E[\mathbf{p}_j\mathbf{p}_l^\dagger] = \frac{1}{N}E\begin{bmatrix} e^{j(\theta_{1j}-\theta_{1l})} & e^{j(\theta_{1j}-\theta_{2l})} & \dots & e^{j(\theta_{1j}-\theta_{Nl})} \\ e^{j(\theta_{2j}-\theta_{1l})} & e^{j(\theta_{2j}-\theta_{2l})} & \dots & e^{j(\theta_{2j}-\theta_{Nl})} \\ \vdots & \vdots & \vdots & \vdots \\ e^{j(\theta_{Nj}-\theta_{1l})} & e^{j(\theta_{Nj}-\theta_{2l})} & \dots & e^{j(\theta_{Nj}-\theta_{Nl})} \end{bmatrix}. \tag{12}$$

Since θ_{mn}s are independent, we have

$$\frac{1}{N}E[e^{j(\theta_{mj}-\theta_{nl})}] = \frac{1}{N}\delta_{(m-n)}\delta_{(j-l)}, \tag{13}$$

where δ_k denotes the Kronecker delta function that evaluates to one only when $k=0$ and zero otherwise. Therefore,

$$E[\mathbf{p}_j\mathbf{p}_l^\dagger] = \frac{\delta_{(j-l)}}{N}\begin{bmatrix} \delta_0 & \delta_{-1} & \dots & \delta_{(1-N)} \\ \delta_1 & \delta_0 & \dots & \delta_{(2-N)} \\ \vdots & \vdots & \vdots & \vdots \\ \delta_{(N-1)} & \delta_{(N-2)} & \dots & \delta_0 \end{bmatrix}. \tag{14}$$

From (14), we have the following:

$$E[\mathbf{p}_j\mathbf{p}_l^\dagger] = \begin{cases} \mathbf{0}_{N\times N} & \text{if} \quad j \neq l, \\ \frac{1}{N}\mathbf{I}_N & \text{if} \quad j = l, \end{cases} \tag{15}$$

where $\mathbf{0}_{N\times N}$ denotes the all zero matrix of size $N \times N$. Therefore, we have $E[g_{ij}g_{kl}^*]$ as

$$E[g_{ij}g_{kl}^*] = \begin{cases} 0 & \text{if} \quad j \neq l, \\ \frac{1}{N}\mathbf{h}_i^\dagger\mathbf{h}_k & \text{if} \quad j = l, i \neq k \\ \frac{1}{N}\|\mathbf{h}_i\|^2 & \text{if} \quad j = l \text{ and } i = k. \end{cases} \tag{16}$$

From (10) and (16), we have

$$\rho_{ij,kl} = \begin{cases} 0 & \text{if} \quad j \neq l, \\ \frac{\mathbf{h}_i^\dagger\mathbf{h}_k}{\|\mathbf{h}_i\|\|\mathbf{h}_k\|} & \text{if} \quad j = l, i \neq k \\ 1 & \text{if} \quad j = l \text{ and } i = k. \end{cases} \tag{17}$$

Further, because of the structure of $\tilde{\mathbf{H}}$,

$$\mathbf{h}_i^\dagger\mathbf{h}_k = \begin{cases} \text{non-zero} & \text{if} \quad \lceil\frac{i}{N_r}\rceil = \lceil\frac{k}{N_r}\rceil \\ 0 & \text{otherwise.} \end{cases} \tag{18}$$

It can be observed from (16) through (18) that the random phase precoding operation makes the correlation coefficients between several pairs of the entries of $\mathbf{G}$ to become zero. Now, consider the ratio of the number of non-zero correlation coefficients to the total number of correlation coefficients, and denote this ratio as α. It can be seen that

$$\begin{aligned} \alpha &= \frac{N_t p^2\binom{N_r}{2}}{\binom{N_r N_t p^2}{2}} = \frac{N_t p^2 N_r(N_r-1)}{N_r N_t p^2(N_t N_r p^2-1)} \\ &= \frac{N_r-1}{N_t N_r p^2-1}. \end{aligned} \tag{19}$$

For large values of p,

$$\alpha \approx \frac{N_r}{N_t N_r p^2} = \frac{1}{N_t p^2}. \tag{20}$$

From (20), we see that for large values of p, the ratio α becomes very small, meaning that most of the correlation coefficients become zero. That is, the effective channel matrix $\mathbf{G}$ becomes increasingly uncorrelated for increasing values of p. This explains the improved performance achieved by the RPP operation even with reduced inter-antenna spacing.

IV. Indexed RPP scheme

In this section, we propose indexed RPP scheme for mmWave MIMO systems. Figure 8 shows the transmitter of the proposed indexed RPP scheme. In this scheme, a set of predefined RPP matrices are indexed to convey additional information bits. The transmitter takes $N_t p$ modulated symbols from a modulation alphabet $\mathbb{A}$ as the input and forms a vector $\mathbf{x}$ of length $N_t p \times 1$. This vector is precoded with an RPP matrix of size $N_t p \times N_t p$ that is chosen from a collection

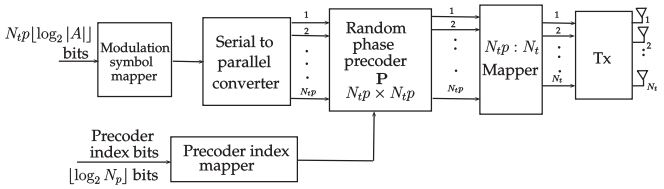

Fig. 8. Indexed RPP scheme.

of predefined precoder matrices. This collection of precoder matrices is a set denoted by $\mathbb{P} = \{\mathbf{P}_1, \mathbf{P}_2, \cdots, \mathbf{P}_{N_p}\}$, where $N_p = |\mathbb{P}|$. Each element of this set is an $N_tp \times N_tp$ matrix with entries as described in Sec. III. The choice of the precoder matrix used to precode the input vector $\mathbf{x}$ conveys $\frac{1}{p}\lfloor \log_2 N_p \rfloor$ information bits per channel use. Hence, the transmission efficiency of indexed RPP scheme is given by

$$\eta = \frac{1}{p}(N_t p \log_2 \mathbb{A} + \lfloor \log_2 N_p \rfloor) \text{ bpcu}. \tag{21}$$

Denoting n as the number of precoder index bits per channel use, i.e., $n \triangleq \frac{1}{p}\lfloor \log_2 N_p \rfloor$, the size of the precoder set is $N_p = |\mathbb{P}| = 2^{np}$. For example, if $p = 2$ and $n = 2$, then $N_p = 2^4 = 16$. The $N_r p \times 1$ received signal vector at the receiver is given by

$$\mathbf{y} = \tilde{\mathbf{H}}\mathbf{P}_j\mathbf{x} + \mathbf{n}, \tag{22}$$

where $\mathbf{P}_j$ is the $N_tp \times N_tp$ RPP matrix chosen from $\mathbb{P}$ and $\tilde{\mathbf{H}}$ is the $N_rp \times N_tp$ matrix as described in Sec. III. The ML detection rule is given by

$$\{\hat{\mathbf{x}}, \hat{j}\} = \underset{\mathbf{x}\in\mathbb{A}^{N_tp},\ j=1,2,\cdots,N_p}{\operatorname{argmin}} \|\mathbf{y} - \tilde{\mathbf{H}}\mathbf{P}\mathbf{x}\|^2. \tag{23}$$

A. Simulation results

In Fig. 9, we present the BER performance of the indexed RPP scheme with $N_t = N_r = 2$, $p = 2$, $N_p = 256$, and BPSK. We compare this performance of indexed RPP with that of RPP without indexing with $N_t = N_r = 2$, $p = 2$, and 8-QAM. The achieved rate in both the systems is 6 bpcu. Further, an inter-antenna spacing of $\frac{\lambda}{2}$ is used in both the systems. The simulations are performed for LOS channel ($K = \infty$) and Rician channel with $K = 10$ dB. Figure 9 shows that the performance of indexed RPP is better than RPP without indexing by about 9 dB in LOS channel and about 2.5 dB in Rician channel with $K = 10$ dB. This can be attributed to the fact that the indexed RPP conveys some bits through the choice of precoder matrix. This allows the use of smaller modulation alphabet in indexed RPP compared to RPP without indexing to achieve the same rate (i.e., BPSK in indexed RPP and 8-QAM in RPP without indexing).

V. Conclusions

We proposed 'random phase precoding' as a novel technique to achieve compact antenna spacing in mmWave MIMO systems. The optimum inter-antenna separation that can result in orthogonal channel matrices under LOS conditions is typically of the order of tens of wavelengths. RPP is a simple and practically implementable technique that allows suboptimum inter-antenna spacing, of the order of wavelength (5 mm at 60 GHz frequency) and yet achieves a performance

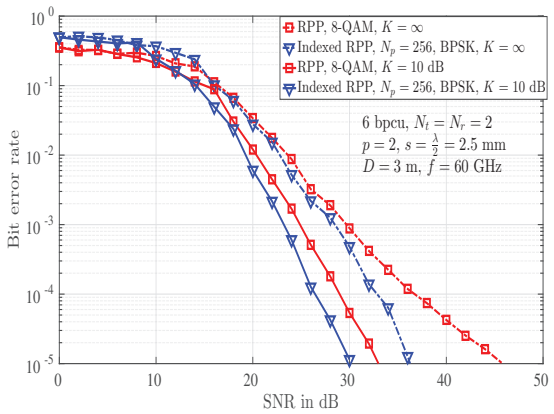

Fig. 9. BER performance of RPP scheme without and with indexing for $\lambda/2$ spaced 2×2 MIMO system at 60 GHz, in LOS channel and Rician channel with $K = 10$ dB, and ML detection.

comparable to that of optimally spaced antenna arrays. This is achieved without the need for channel state information at the transmitter. We also showed analytically that RPP reduces the correlation in the effective channel. We then proposed an indexed RPP scheme that uses a collection of predefined RPP matrices and the choice of precoder matrix used conveys additional information bits. Numerical results showed that the proposed indexed RPP scheme can outperform RPP without precoder indexing.

References

[1] T. S. Rappaport, R. W. Heath, Jr., J. N. Murdock, and R. C. Daniels, *Millimeter Wave Wireless Communications*, Prentice Hall, 2014.

[2] Y. Niu, Y. Li, D. Jin, L. Su, and A. V. Vasilakos, "A survey of millimeter wave (mmWave) communications for 5G: opportunities and challenges," *Wireless Networks*, vol. 21, no. 8, pp. 2657-2676, Aug. 2015.

[3] A. L. Swindlehurst, E. Ayanoglu, P. Heydari, and F. Capolino, "Millimeter-wave massive MIMO: the next wireless revolution?," *IEEE Commun. Mag.*, vol. 52, no. 9, pp. 56-62, Sep. 2014.

[4] I. Sarris and A. R. Nix, "Design and performance assessment of high-capacity MIMO architectures in the presence of a line-of-sight component," *IEEE Trans. Veh. Tech.*, vol. 56, no. 4, pp. 2194-2202, Jul. 2007.

[5] F. Bohagen, P. Orten, and G. Oien, "Design of optimal high-rank line-of-sight MIMO channels," *IEEE Trans. Wireless Commun.*, vol. 6, no. 4, pp. 1420-1425, Apr. 2007.

[6] C. Sheldon, E. Torkildson, M. Seo, C. P. Yue, M. Rodwell, and U. Madhow, "Spatial multiplexing over a line-of-sight millimeter-wave MIMO link: a two-channel hardware demonstration at 1.2Gbps over 41m range," *Proc. European Wireless Tech. Conf.*, pp. 198-201, Oct. 2008.

[7] C. Sheldon, M. Seo, E. Torkildson, M. Rodwell, and U. Madhow, "Four-channel spatial multiplexing over a millimeter-wave line-of-sight link," *Proc. Intl. Microwave Symp.*, pp. 389-392, Jun. 2009.

[8] P. Liu and A. Springer, "Space shift keying for LOS communication at mmWave frequencies," *IEEE Wireless Commun. Lett.*, vol. 4, no. 2, pp. 121-124, Apr. 2015.

[9] P. Liu, M. Di Renzo, and A. Springer, "Line-of-sight spatial modulation for indoor mmWave communication at 60 GHz," *IEEE Trans. Wireless Commun.*, vol. 15, no. 11, pp. 7373-7389, Nov. 2016.

[10] K. Wiklundh and G. Eriksson, "A study of the capacity for different element spacing on compact MIMO platforms," *Proc. IEEE PIMRC'2008*, pp. 1-5, Sep. 2008.

[11] R. Annavajjala and P. V. Orlik, "Achieving near exponential diversity on uncoded low-dimensional MIMO, multi-user and multi-carrier systems without transmitter CSI," *Proc. ITA'2011*, Jan. 2011.

[12] T. Lakshmi Narasimhan, Y. Naresh, T. Datta, and A. Chockalingam, "Pseudo-random phase precoded spatial modulation and precoder index modulation," *Proc. IEEE GLOBECOM'2014*, pp. 3868-3873, Dec. 2014.

[13] J. Sarris and A. R. Nix, "Rician K-factor measurements in a home and an office environment in the 60 GHz band," *Proc. Mobile and Wireless Commun. Summit*, Jul. 2007.